Dark Matter and Dark Energy: Cosmology of Spacetime with Surface Tension [DRAFT]

H A Perko[1]
[1]Office 14, 140 E. 4th Street, Loveland, CO, USA 80537

E-mail: hperko@kopparesearch.com, howie@colostate.edu

Abstract. A mechanical model of spacetime was introduced at a prior conference for describing perturbations of stress, strain, and displacement within a spacetime exhibiting surface tension. In the introductory presentation, it was shown that equations governing metric dynamics provide an alternate geometric formulation for quantum mechanics. Analogies were drawn between micro-perturbations in spacetime and the wave equations of quantum mechanics. At a second conference, the model was extended to include gravity by proposing an anisotropic coupling tensor to relate stress-energy and curvature instead of the scalar Einstein constant.

In this presentation, the model is applied to cosmology. It is shown that the tensor equations describing spacetime with surface tension can be rearranged such that they contain components resembling dark matter and dark energy. This form of the model is compared with galaxy rotation curves. It is shown that surface tension causes flattening of rotation curves. The model is also evaluated using Friedman Robertson Walker metrics. It is shown that surface tension tends toward a flat, homogeneous, isotropic universe geometry. It is suggested that dark matter and dark energy are the cosmological manifestations of surface tension in spacetime.

1. Introduction

Many physicists believe that gravity and quantum mechanics eventually will be unified under a single theory. Earlier works on unification aimed to "geometrize" the electromagnetic field. Some approaches connected an additional linear form to the metric (Weyl), expanded the dimensionality of space (Kaluza), suggested an asymmetric Ricci Tensor (Eddington), added an antisymmetric tensor to the metric (Bach, Einstein), and replaced the metric by a 4-bein field (Einstein) [1]. More recent approaches to unification include string theory and M-theory [2,3], stochastic mechanics [4], geometric field theory of electrodynamics [5,6,7], and many others.

The approach being evaluated here began by trying to answer a simple question, how would nature construct small particles from the geometry of spacetime itself? The proposed answer draws upon known concepts from physical chemistry to introduce surface tension to spacetime [8-12]. From everyday experiences, we know that surface tension has a predominant role in the physics of small objects. In a similar way, it was argued in [8-12] that incorporating surface tension into general relativity may help build a bridge to quantum mechanics.

The proposed introduction of surface tension to spacetime [8-12] can be summarized by the following arguments: 1.) thermodynamics of surface tension requires negative terms in the spatial diagonal of the stress energy tensor, and 2.) both gravitational and high-energy fields can be combined into one geometry by replacing the traditional gravitational constant by an anisotropic invertible coupling tensor. Making these changes to general relativity allows for the creation of various small particles and quantizes spacetime according to Plank's constant. The wave equations for these systems resemble basic field equations in quantum mechanics wherein interpreted probability waves are replaced by strain and displacement fields in the fabric of spacetime itself.

The question addressed in this paper is how the proposed changes to general relativity would affect cosmology. Simple algebraic manipulation of surface tension tensor equations produces a form of general relativity that resembles two of the most widely accepted and yet unexplained aspects of mainstream cosmology, dark matter and dark energy. Many are working to explain dark matter and dark energy phenomena through modifications to the equations of general relativity (see for example [13-17]). Surface tension of spacetime provides an alternative explanation for dark matter and dark energy.

This paper summarizes the surface tension model of spacetime [8-12] including the underlying thermodynamics and the postulated stress energy tensor with negative spatial terms. It is shown that the stress energy tensor can be rearranged in a way that has terms resembling dark matter and dark energy in cosmology. The rearranged term for dark matter differs from ordinary mass in that it has a scalar potential energy field and would yield flat velocity curves at astronomical distances. The rearranged term for dark energy is a negative cosmological constant that produces a flat and expanding spacetime in FRW cosmology.

2. Geometry

A coordinate system is created by an observer in order to record the position of objects, particles, or events as well as their mass, velocity, electric charge, magnetic field, and other properties relative to the observer. A coordinate system is a record of position in spacetime relative to a single clock.

Making an observation creates a map between the observer and different points or events in a manifold. Other observers create different maps of the same manifold relative to their own coordinate system with their own clock. Relativity teaches that the coordinate systems of all observers are Lorentz transformations of the same manifold. Said another way, coordinate frames at different velocities are rotations by an imaginary angle of the same tensor equations.

It is well known that observers disagree on simultaneity of events. For this reason, the word "simultaneous" has become near synonymous with misunderstanding relativity. This bias is so great that the simultaneity of an observer (coordinate system with one clock) with events and objects in its present time is approached with skepticism. However, the simultaneity of energy, matter, and events at an instant of time IS the very nature of a coordinate system comoving with a single clock. The concept of one clock per observer is important to this work because, as is discussed here in detail, it is the simultaneity of energy in any arbitrary reference frame that manifestly causes spacetime surface tension.

Let us define an observer's 4-dimensional coordinate system by $x^{\mu} \in \mathfrak{M}$, where $x^{\mu} = (x^0, x^1, x^2, x^3)$ and $x^0 = f(t)$. A plot of matter and energy as "seen" by an arbitrary observer is depicted in Figure 1. Each point represents some concentration of matter or energy like an atom, dust grain, star, or galaxy – depending on scale. Each point may be moving at a different velocity within the coordinate system. Matter and energy are dispersed through the observer's space and confined to an infinitesimally thin instant of time as read on the observer's clock upon making an observation.

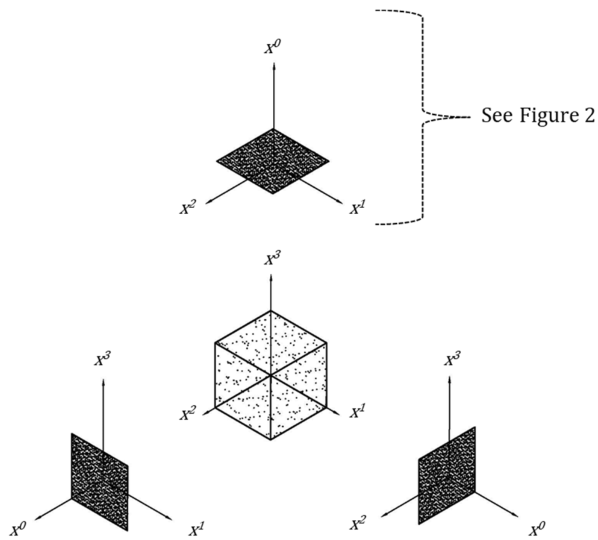

Figure 1. Four-Dimensional Depiction of Matter and Energy as "Seen" in by an Arbitrary Observer

One of the three surfaces in time and two coordinates of space from Figure 1 is depicted in Figure 2. According to general relativity, the observer's coordinate system would have some curvature caused by the density and distribution of mass energy. Thus, the surface in Figure 2 is shown to be undulating and irregular.

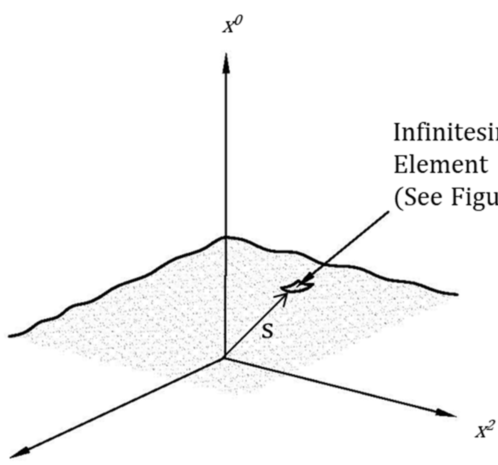

Figure 2. Spatial 3-Surface Exhibiting Curvature due to Energy Contained Therein

3. Surface Tension

A fundamental principle of physical chemistry is that a surface of energy must have surface tension [18]. Physical chemists [18] use a very simple mechanical analogy to explain this principle. Consider the mechanical model in Figure 3. The model consists of a wire frame window with one moveable side and some density of stored surface energy, ♀, dispersed across the opening. In thermodynamic terms, the window represents quantum fields in the present that can affect the probability of future states. The fact that these states are organized in an increment of coordinate time is a higher order (lower entropy) than complete temporal dispersion (loss of causality, faster than light travel, future states affecting the present). The energy required to maintain this lower entropy is stored surface energy. The work done on the system by opening the window some discrete amount is given by,

$$Work = \female dA$$

which for this system with one moveable side can be written,

$$Work = \female Ldx$$

where $dA = Ldx$ represents the additional surface area. Now, given the definition of work is force times length, it appears that ♀ in the second formulation is a tension force per unit length or *surface tension*. Thus, surface tension and surface energy are mechanically equivalent concepts in the physical chemistry of surfaces. This postulate holds regardless of dimensionality of the surface. It holds even for a spatial 3-surface at an instant of coordinate time.

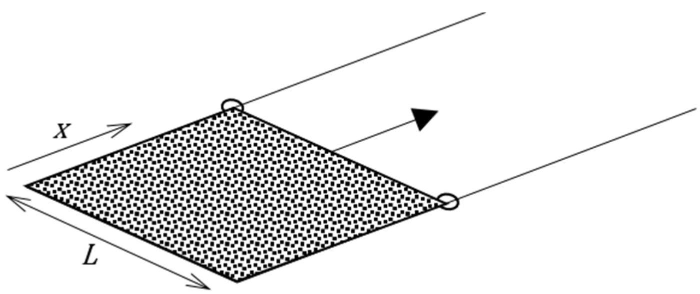

Figure 3. Surface Energy Stretched Across a Wire Frame Window with One Moveable Side

The simple model used by physical chemists for a two-dimensional surface can be mathematically adapted to a 3-surface in relativity. The approach taken is to borrow techniques from continuum mechanics which build a set of coordinate-independent tensor equations to describe the configuration manifold, stress energy states, and the rate of deformation of the energy 3-surface. An infinitesimal element (a discrete point) of 3-surface from Figure 2 is enlarged in Figure 4. The infinitesimal element's frame (also called material coordinates or tangent space) can be described by coordinates, y^ν. The frame of the infinitesimal point is mapped to the observer's coordinates, x^ν, by the four velocity, $\boldsymbol{u}$, with components, $u^{\nu} = \frac{\partial x^{\nu}}{\partial s}$, where s is the spacetime separation between observer and the point (particle or event).

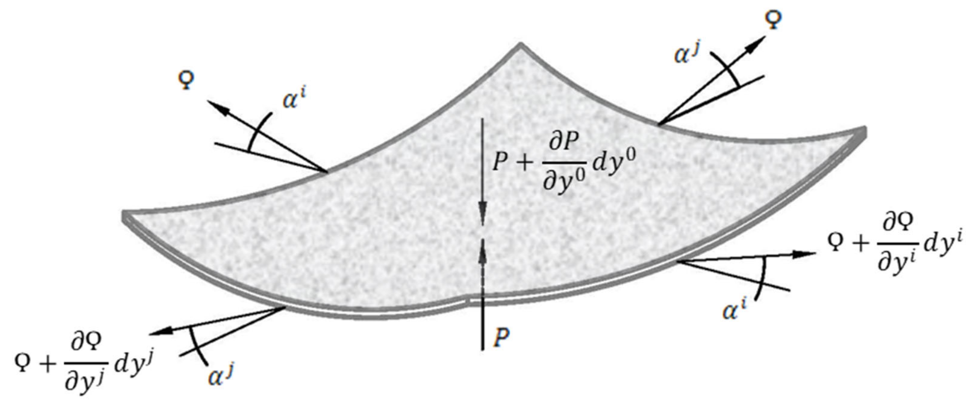

Figure 4. Infinitesimal Element of Spacetime with Matter-Energy Density, P, and Surface Tension, Ϙ

The stress energy tensor for a point in a spacetime continuum in the principle frame of the tangent space at the infinitesimal element point is,

$$T_{\mu\nu} = \begin{bmatrix} dP & 0 & 0 & 0 \\ 0 & -Ϙ & 0 & 0 \\ 0 & 0 & -Ϙ & 0 \\ 0 & 0 & 0 & -Ϙ \end{bmatrix} \qquad (1)$$

Surface tension, Ϙ, is a tensor field, $Ϙ_{ij}$, whose components may vary. However, in the case of spatially flat fluid space, where torsion and shear stresses (off diagonal spatial terms) are zero, then surface tension, Ϙ, is a constant. The spatially flat fluid space with uniform surface tension is assumed herein to be consistent with usual assumptions of physical chemistry of surfaces, unless otherwise noted.

The total energy, W, of a three-surface is,

$$W = \oiint_{\sigma} -Ϙ d\sigma \qquad (2)$$

From the definition of work, the stored energy of a three volume is,

$$W = \oint_{V} dPdV \qquad (3)$$

When combined together through conservation of work and energy, (2) and (3) become,

$$\oiint_{\sigma} -Ϙ d\sigma = \oint_{V} dPdV \qquad (4)$$

According to the divergence theorem,

$$\oiint_{\sigma} ♀ d\sigma = \oint_{V} (\nabla \cdot ♀)\, dV \qquad (5)$$

which means by direct comparison of (4) and (5),

$$\nabla \cdot ♀ = -dP \qquad (6)$$

Differential temporal pressure (mass energy) is the spatial divergence of surface tension.

This line of logic is somewhat analogous to the treatment of corpuscular, capillary, and meniscus geometry in physical chemistry of surfaces. An example of corpuscular geometry is shown in Figure 5. For two-dimensional curved surfaces, surface tension acts against differential surface pressure, dP.

$$\left.\begin{aligned} ♀\, 2\pi R &= dP\, \pi R^2 \\ \frac{2♀}{R} &= dP \end{aligned}\right\} \textit{2-D Surface in 3-Space}$$

From this analogy, one can intuitively derive a similar relationship for spatial three-surfaces intrinsic in time,

$$\left.\begin{aligned} ♀\, 4\pi R^2 &= dP\, \frac{4}{3}\pi R^3 \\ \frac{3♀}{R} &= dP \qquad (7) \end{aligned}\right\} \textit{3-D Surface in 4-Space}$$

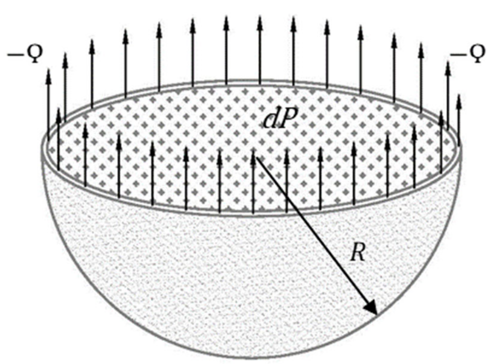

Figure 5. Corpuscle Analog of the Divergence Theorem in Physical Chemistry of Surfaces

4. Unit Transformations

Work in general relativity is generally performed in units where *c=1*. Consider the proper 4-dimensional coordinate system of $x^{\mu} \in \mathfrak{M}$, where $x^{\mu} = (x^0, x^1, x^2, x^3)$ and $x^0 = ct$. In order for the laboratory observer to unravel the units of this coordinate system so that they may use using a common chronometer, the time-time term of the stress energy tensor should be multiplied by c^2. The time-space components in the first column and top row of the stress energy tensor should be multiplied by c and the spatial components by *1*. Thus, a proper conversion of units is accomplished by the coordinate transformation,

$$T'^{(x'^0=t)}_{\mu\nu} = (C_{\mu\nu}) \circ (T^{(x^0=ct)}_{\mu\nu})$$

where $T^{(x^0=ct)}_{\mu\nu}$ is the stress energy tensor in c=1 units, $T'^{(x'^0=t)}_{\mu\nu}$ is the prime stress energy tensor in laboratory units, and

$$C_{\mu\nu} = \begin{bmatrix} c^2 & c & c & c \\ c & 1 & 1 & 1 \\ c & 1 & 1 & 1 \\ c & 1 & 1 & 1 \end{bmatrix}$$

is the coordinate transformation. In this notation the symbol ◦ indicates the Hadamard product which is a term-by-term or point-wise product. To those accustom to Einstein notation, this type of coordinate transformation might appear inappropriate, because there is an imbalance of dependent indices. When taking the Hadamard product, Einstein summation is not implied. This transformation is legitimate in relativity as the speed of light, and hence the basis of transformation, is constant for all reference frames. In this work, parentheses are used along with ◦ to indicate the Hadamard product.

The transformation $C_{\mu\nu}$ is symmetric. None of the terms in $C_{\mu\nu}$ are equal to zero, so it is invertible by Hadamard rules and the product $(C_{\mu\nu}) \circ (C_{\mu\nu})^{-1}$ is equal to the Hadamard identity matrix,

$$\begin{bmatrix} 1 & 1 & 1 & 1 \\ 1 & 1 & 1 & 1 \\ 1 & 1 & 1 & 1 \\ 1 & 1 & 1 & 1 \end{bmatrix}$$

Applying this transformation to both sides of the equation of general relativity modifies units of $T_{\mu\nu}$ and the geometric curvature tensor and is a consistent way to switch back and forth between dimensional forms. Thus, in prime laboratory units, the relationship between surface tension and mass energy (7) is given by,

$$\frac{3♀'}{R} = \frac{dP'}{c^2} \qquad (8)$$

4. Dark Matter and Dark Energy

Simply by adding and subtracting ♀ from the time-time term, the stress-energy tensor, [1], with surface tension can be rewritten as,

$$T_{\mu\nu} = \begin{bmatrix} dP + ♀ & 0 & 0 & 0 \\ 0 & 0 & 0 & 0 \\ 0 & 0 & 0 & 0 \\ 0 & 0 & 0 & 0 \end{bmatrix} - ♀ g_{\mu\nu} \qquad (9)$$

In this form, surface tension appears as an additional mass term, +Ϙ, and a negative cosmological constant, -Ϙ$g_{\mu\nu}$. The additional mass term could be interpreted as "dark matter" and the negative cosmological constant as "dark energy" in cosmology applications. Ordinary luminous matter, *dP*, and "dark matter", +Ϙ, are interrelated by (6) and (8) of the previous section. A correspondence between luminous matter and dark matter is to be expected. Eloquent arguments for such a correspondence are given in [19].

5. Orbital Velocities

In this section, the gravitational field around a galaxy or other massive astronomical object is derived following similar steps as Albert Einstein's famous 'Newton's Theory as a First Approximation' [20] with the extra rearranged surface tension "dark energy" term, +Ϙ, included. Suppose that the metric of spacetime at some distance, *R*, from the center of a galaxy differs from flat by a small amount due to a gravitational field generated exclusively by matter in the finite region of the galaxy and its corresponding surface tension. If the velocities of stars within and around the galaxy are small as compared with the speed of light, then spatial components of general relativity become insignificant and the gravitational field is quasi-static. With these assumptions, the general relativity equivalent of Newton's law of gravitation around a galaxy with surface tension becomes,

$$\frac{1}{c^2}\frac{d^2x_\tau}{dt^2} = -\frac{1}{2}\frac{\partial g_{00}}{\partial x_\tau} \qquad (10)$$

$$\nabla^2 g_{00} = \frac{8\pi G}{c^2}(dP' + \text{Ϙ}')$$

where $\tau = 1,2,3$ and differential temporal pressure, *dP*, is in units of mass density. Given the relationship (8), the second equation above is replaced by,

$$\nabla^2 g_{00} = \frac{8\pi G}{c^2}\left(dP' + \frac{rdP'}{3c^2}\right) \qquad (11)$$

From Gauss' law,

$$\oint_V \nabla^2 g_{00}\,dV = \oint_V (\nabla\cdot\nabla g_{00})dV = \oiint_\sigma \nabla g_{00}\cdot d\sigma \qquad (12)$$

Substituting (10) and (11) into (12) yields,

$$\frac{8\pi G}{c^2}\int_0^{2\pi}\int_0^{2\pi}\int_0^R \left(dP' + \frac{rdP'}{3c^2}\right) r^2 Sin\varphi d\varphi d\theta dr = -\int_0^{2\pi}\int_0^{2\pi}\frac{2}{c^2}\frac{d^2x_\tau}{dt^2}R^2 Sin\varphi d\varphi d\theta \qquad (13)$$

$$\frac{8\pi G}{c^2}\,4\pi\int_0^R\left(dP' r^2 dr + \frac{dP'}{3c^2}r^3\right)dr = -\frac{8\pi}{c^2}\frac{d^2x_\tau}{dt^2}R^2$$

$$G\,4\pi\left(\frac{dP'}{3}R + \frac{dP'}{12c^2}R^2\right) = -\frac{d^2x_\tau}{dt^2}$$

Let mass density, dP', equal galaxy mass contained in a sphere of radius R divided by volume of that sphere (e.g. $dP'=3M/4\pi R^3$) and solve (13) to obtain,

$$G\,4\pi\left(\frac{M}{4\pi R^2}+\frac{3M}{48\pi Rc^2}\right)=-\frac{d^2x_\tau}{dt^2}$$

which reduces to Newton's equation for gravitational acceleration with surface tension,

$$-G\left(\frac{M}{R^2}+\frac{M}{16Rc^2}\right)=\frac{d^2x_\tau}{dt^2} \qquad (14)$$

Note that the second term on the left side of (14) is dimensionless. See the Discussion section for more information on units.

The orbital velocity of stars around a galaxy, v, is related to gravitational acceleration by,

$$\frac{v^2}{R}=-\frac{d^2x_\tau}{dt^2} \qquad (15)$$

Hence, from (14) and (15) orbital velocity is given by,

$$v=\sqrt{GM\left(\frac{1}{R}+\frac{1}{16c^2}\right)}$$

If a galaxy or orbiting system has an axis of rotation at an angle, i, relative to the observer's line of sight, then a correction must be made to the velocity. The corrected orbital velocity is given by,

$$v_r=\sin i\sqrt{GM\left(\frac{1}{R}+\frac{1}{16c^2}\right)} \qquad (16)$$

The parameter i is called inclination. When a galaxy is at an inclination of 0 degrees, the observer's line of sight is directly in-line with the axis of rotation, the galaxy is being viewed "head-on", none of the orbital velocity is towards the observer, and no Doppler velocity difference is measured. When a galaxy is at an inclination of 90 degrees, the axis of rotation is perpendicular to the line of sight, the galaxy is being viewed "on-edge", and Doppler shift measurements provide the correct orbital velocity.

6. Galaxy Rotation Curves

To test the validity of the surface tension model, the predicted orbital velocity from (16) is compared with astronomical measurements for three example galaxies. The first is NGC 2903, an approximately 30 kpc diameter barred spiral galaxy located about 7,600 kpc from Earth in the constellation Leo. The second is NGC 3198, an approximately 35 kpc diameter barred spiral galaxy located about 13,800 kpc from Earth in the constellation Ursa Major. The final is M31, also known as the Andromeda galaxy, Messier 31, or NGC 224, is a 67 kpc diameter barred spiral galaxy located only 779 kpc from Earth in the constellation Andromeda. Basic properties of these galaxies are shown in Table 1. For this work, orbital velocities from astronomical measurement of Doppler shifts were obtained from [21] for the first two galaxies and from [22] for M31.

Table 1. Properties of Subject Galaxies

Galaxy	Diameter	Distance	Mass (CG)	Mass (♀)	Inclination	Luminosity
	kpc	*kpc*	*Mo*	*Mo*	*deg*	*Lo*
2903	30	7600	7.10E+10	4.0E+08	62	3.87E+10
3198	35	13800	4.95E+10	2.4E+08	66	2.45E+10
M31	67	779	1.50E+12	2.7E+08	77	2.60E+10

In order to compare predicted orbital velocity from (16) with astronomical measurements, luminous matter density of the galaxy must be estimated. Current estimates of luminous matter density found in many cosmology references are biased, because they were generated in-part by curve fitting galaxy rotation curves to Newton's gravity [13]. To avoid any bias for this comparison, astronomical measurements of surface brightness were used to directly estimate luminous matter density as a function of radial distance from the galaxy center.

Surface brightness data for the galaxies under consideration were found in [23] and [24]. An example of one of the surface brightness profiles from [23] for the galaxy NGC 2903 is reproduced in Figure 6. The various dashed and solid lines in the top chart represent surface brightness measured in J, H, and K bands and 2MASS. The bottom chart shows stellar mass-to-light ratio. The thin line represents mass-to-light ratio based on galaxy formation models in J-K bands and the thick line is from 3.6 μm emission data scaled down by the diet Salpeter correction. The diet Salpeter correction is biased, because it is understood to be derived from curve fitting to match Newton's gravity. In this work, surface brightness measurements in the J band was used along with the unscaled J-K band stellar mass-to-light ratio. The J band was selected, because it is where the spectrum of the sun and various galaxies overlap with greatest brightness. For the M31 galaxy, J band surface brightness is not presented in [24] so the I band was used as it is the next closest band.

The ratio of flux density, F, coming from a discrete area of galaxy relative to the flux density, F_0, that would be measured if a single star with luminosity of the Sun were located at the same distance from Earth, $\frac{F}{F_0}$, provides the number density, n, of equivalent Suns in the galaxy at that location. Flux density is quantified in astrophysics by surface brightness on a log base 10 scale and is typically given in units of magnitudes per square arcsecond. The ratio, $\frac{F}{F_0}$, can be obtained from surface brightness in the following way,

$$\mu - \mu_0 = -2.5 \log_{10}\left(\frac{F}{\alpha^2}\right) + 2.5 \log_{10}\left(\frac{F_0}{\alpha^2}\right)$$

$$\mu - \mu_0 = -2.5 \log_{10}(n) \qquad (17)$$

where μ is the total measured surface brightness of an area, and μ_0 is the reference surface brightness of that same area if it were illuminated by a single star equivalent to the Sun. The visual angle, α, defining the discrete area of sky cancels from the logarithm. Reference surface brightness, μ_0, is found from,

$$\mu_0 = -2.5\ \log_{10}\left(\frac{F_0}{\alpha^2}\right) = -2.5\ \log_{10}\left(\frac{L_\odot}{4\pi d^2}\frac{d^2}{D^2}\frac{\pi^2}{180^2 60^4}\right)$$

$$\mu_0 = -2.5\ \log_{10}\left(\frac{L_\odot}{4\pi D^2}\right) - 2.5\log_{10}\left(\frac{\pi^2}{180^2 60^4}\right)$$

$$\mu_0 = -2.5\ \log_{10}\left(\frac{L_\odot}{4\pi D^2}\right) + 26.6 \qquad (18)$$

where $L_\odot$ is solar luminosity, d is the distance to the galaxy, D is the length of galaxy subtended by the angle α, and the ratio $\frac{d^2}{D^2}$ is the small angle approximation of α^2, since $\frac{d}{D} = \tan\alpha \approx \alpha$ in radians. The constants consisting of π, 180, and 60 convert the square angle in radians to arcseconds^2. The expression can be further simplified by introducing the absolute magnitude of the Sun, M_0, which is a measure of the flux density from the Sun if it were placed at a distance of 10 pc from the earth.

$$M_0 = -2.5\ \log_{10}\left(\frac{L_\odot}{4\pi 10^2}\right) \qquad (19)$$

Adding and subtracting the different expressions for absolute magnitude (19) from (18), yields

$$\mu_0 = -2.5\ \log_{10}\left(\frac{L_\odot}{4\pi D^2}\right) + 26.6 + M_0 + 2.5\ \log_{10}\left(\frac{L_\odot}{4\pi 10^2}\right)$$

$$\mu_0 = -2.5\ \log_{10}\left(\frac{L_\odot}{4\pi D^2}\frac{4\pi 10^2}{L_\odot}\right) + 26.6 + M_0$$

$$\mu_0 = -2.5\ \log_{10}\left(\frac{10^2}{D^2}\right) + 26.6 + M_0$$

which, for D^2=1 pc^2, becomes simply,

$$\mu_0 = 21.6 + M_0 \qquad (20)$$

Thus, (17) can be rearranged with (20) to find the number density, n, of equivalent Suns in a 1 pc^2 area of galaxy. Absolute magnitude, M_0, varies by light frequency band width and should be matched to the surface brightness measurement. Based on [25] and a supplemental internet search, the absolute magnitude of the Sun in this study is taken to be 3.87 in the J-band and 4.11 in the I-band.

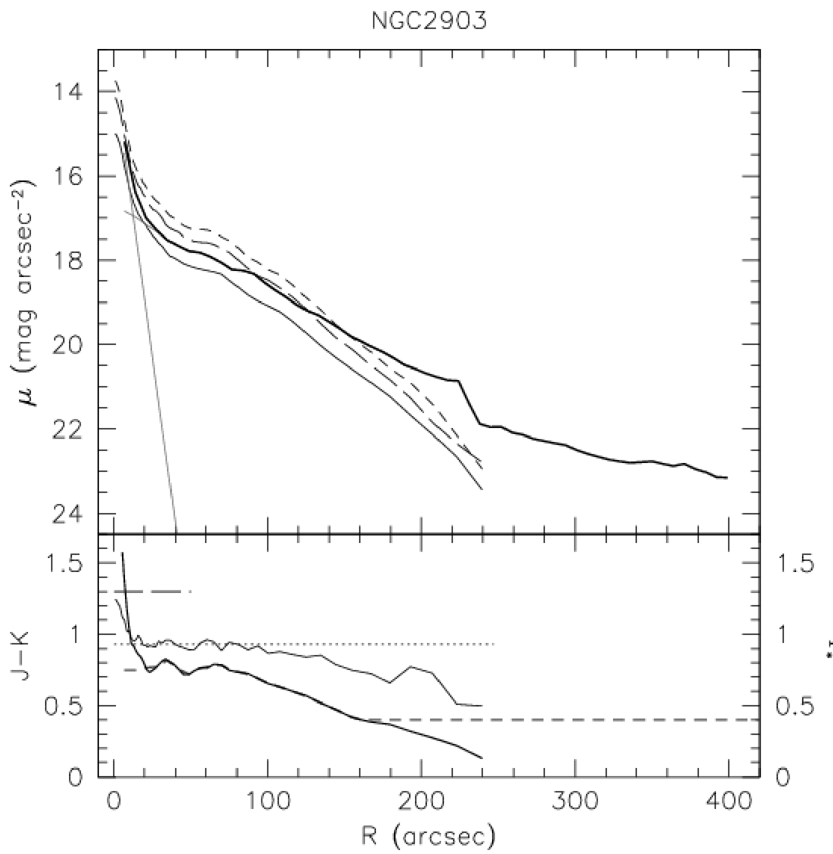

Figure 6. Surface Brightness of NGC2903 [23]

The subtotal gravitational luminous mass, *M*, located within a distance, *R*, from the center of a galaxy can be approximated by integrating the number density as a function of radial distance, n(r), thus,

$$M(R) = 2\pi\, \Upsilon M_{\odot} Cos\ i \int_0^R n(r) r dr \qquad (18)$$

where Υ is the mass-to-light ratio from [23] and [24], *i* is inclination angle, and $M_{\odot}$ is solar mass. This integration was performed for each galaxy by summing calculated number density over discrete radii. The resulting discretized mass values, *M(R)*, were then inserted into (16) to obtain predicted orbital velocity with surface tension. The initial fit to measured rotational velocity data was poor. The shape of the fit was intriguing, but (16) overpredicted orbital velocity by a factor of 10.

Subsequently, the discretized mass values from (18) were multiplied by a single fitting parameter in an attempt to provide a better correlation. Results of this fit are shown in Figures 7 through 9. Predicted velocity from the model is shown by the solid white line. Measured galaxy rotation curves from [21] and [22] are shown by the yellow dots for comparison. The dashed line near the bottom of each chart is the orbital velocity predicted by Newton based on the fitted number density. As can be seen, the fit of the model to the shape of rotational velocity curves for these three galaxies is intriguing.

Interestingly, the best-fit for all three galaxies was obtained by correcting (18) by multiplying each mass increment by a constant, φ, unique to each galaxy such that the resulting overall mass-to-light ratio equals exactly 1%. Overall mass-to-light ratio is defined here as total mass of the galaxy from (18) times a single constant divided by the published total luminosity from Table 1. In other words, the fitting constant, φ, could be determined for all three galaxies by assuming an overall mass-to-light ratio of 1/100, thus

$$\frac{1}{100} = \frac{\varphi \int M(R)dR}{L} \qquad (19)$$

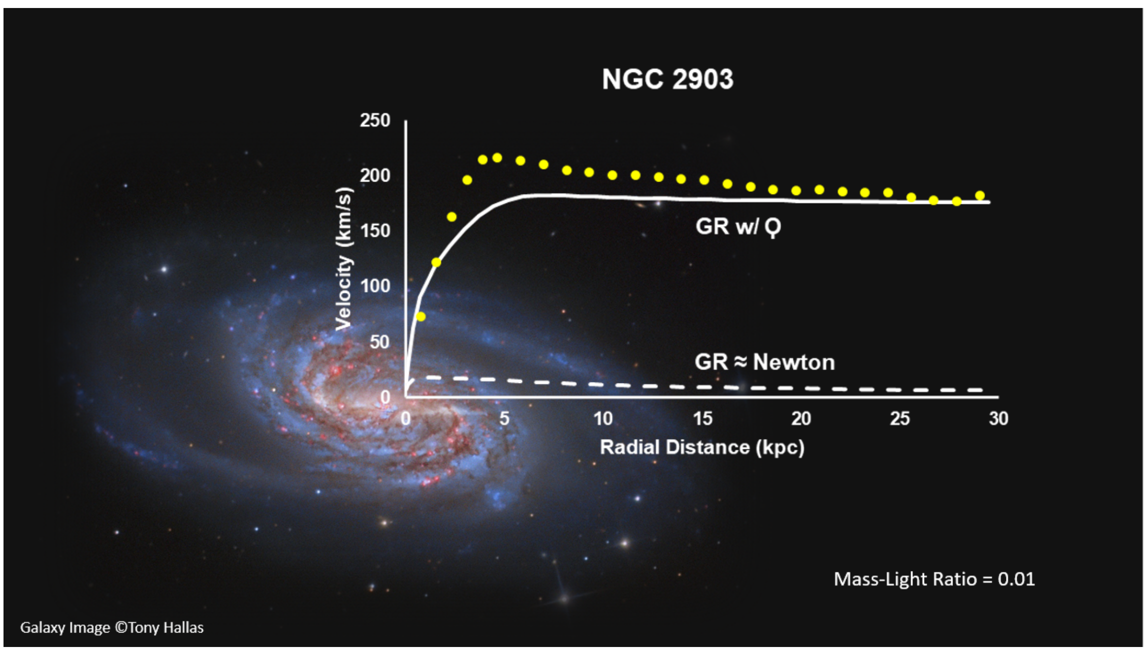

Figure 7. Predicted and Measured Galaxy Rotation Curves for NGC2903

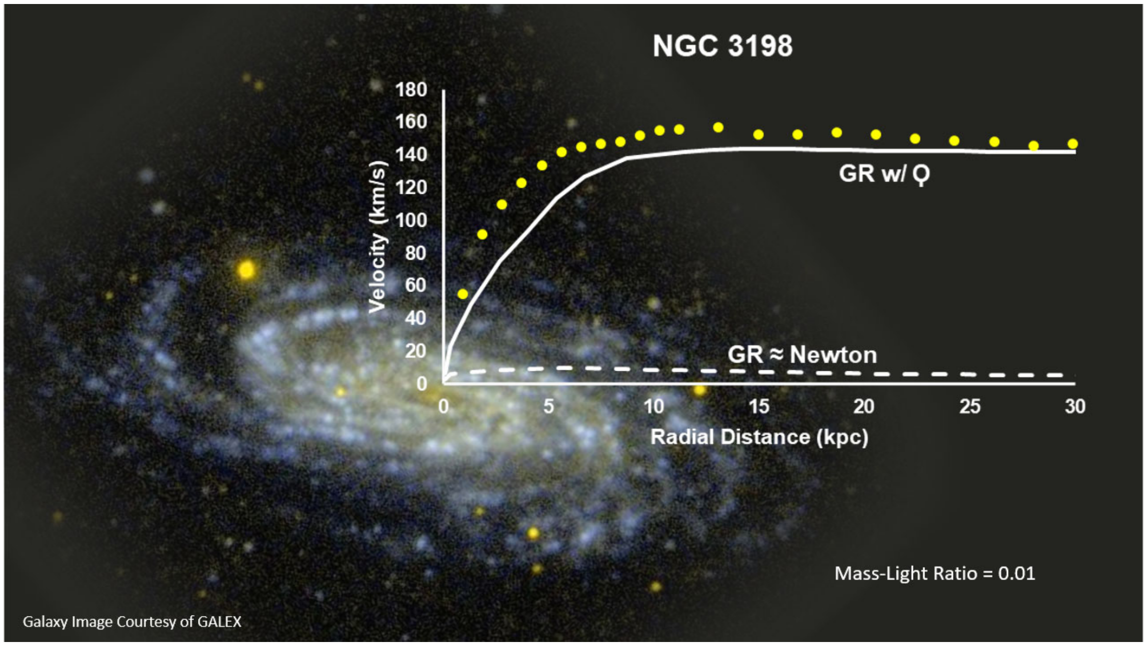

Figure 8. Predicted and Measured Galaxy Rotation Curves for NGC3198

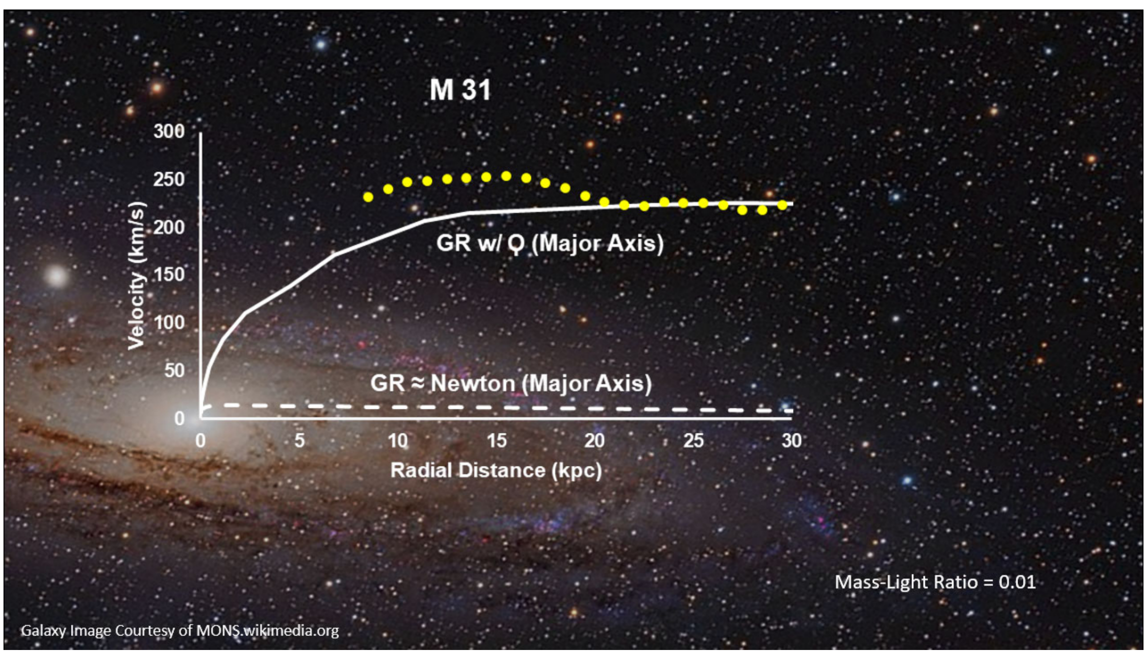

Figure 9. Predicted and Measured Galaxy Rotation Curves for M31

Using (19), values of φ were determined to be 0.01, 0.004, and 0.023 for NGC 3198, NGC 2903, and M31, respectively. The reason φ is 0.01 for NGC 2903 is that the generally accepted mass-to-light ratio for this galaxy is close to 1.0, whereas the generally accepted mass-to-light ratio for the other two galaxies is much different than unity so some additional correction is needed to bring those data into correlation with an overall mass-to-light ratio of 0.01.

7. Tully-Fisher Relation

The surface tension model predicts orbital velocities approaching a constant at large distance from galactic centers. This asymptotic velocity is a function of galactic luminous mass only. In this section, the model will be compared to the Tully-Fisher relation and contrasted with predictions from leading MOND theories.

{this section forthcoming}

8. Hubble Universe

In this section, the model will be evaluated with regard to the "dark energy" or negative cosmological constant. FRW equations with surface tension are derived and compare with the Hubble Constant.

{this section forthcoming}

9. Discussion

The fact that the same overall mass-to-light ratio caused best-fit of the theoretical surface tension model to the data for all three galaxies despite a wide range in overall mass, distance from Earth, total luminosity, and structure of the test subjects suggests the surface tension model has some merit and deserves further study. A constant correction adds credence to the model predictions. However, the exact nature of this constant discrepancy is unknown at this time and needs to be determined. One astrophysical explanation is that, if the model and its application to the data are correct, then stars located in the bulge, which makes up most of the mass of galaxies, are actually 100 times more luminous by mass as compared to the Sun. Another possible explanation is that there is a systemic mathematical error in the derivation or in the application of the model. For example, the correction of 1/100 is exactly equal to $(1/10\ \text{pc})^2$, the standard distance used to calculate absolute magnitude. If the surface brightness data obtained from [23] and [24] were somehow corrected for absolute magnitude instead of apparent magnitude, then such a correction could explain the constant variation. Of course, another explanation is that the surface tension model itself is incorrect and that the best fit obtained here is some sort of accident. More work and the modeling of many more galaxies is needed to find the answer.

It should be noted that the proposed model is affected to small extent by referenced distance to galaxy, referenced absolute solar magnitude, and surface brightness band variations. Corrections were made for inclination. Redshift received consideration, but preliminary calculations suggested none of these parameters could explain the systematic variance between model predictions and measured rotational curves. Background surface brightness of more distant celestial objects located beyond the subject galaxies was evaluated. Accounting for background brightness seems to make predicted velocity curves trend downward. Taking into account background surface brightness could explain the shape of the measured rotation curve in Figure 7, but here again does not seem to explain the constant variance between model predictions and measurements. It is possible that reference surface brightness should be attenuated by scattering and/or absorption phenomena but that would increase calculated mass and worsen the correlation.

One of the most encouraging aspects of the fit between the model and measured galaxy rotation curves is the shape of the predicted curves. The addition of hypothetical dark matter to Newton gravity allows one to correct the shape of Newtonian rotation curves so that they do not drop off at $1/r^{1/2}$, but no amount of configuration of dark matter can explain the discrepancy in the initial slope of rotation curves. Figure 10 is a duplication of Figure 7 except with overall mass-to-light ratio set to 1.0. As can be seen in the figure, Newton gravity not only does not match rotation curves at large distances, it overpredicts the initial slope of the rotation curve. The surface tension model not only corrects rotation curves at large radii, it also tends to flatten the initial rotation curve resulting in an overall better fit.

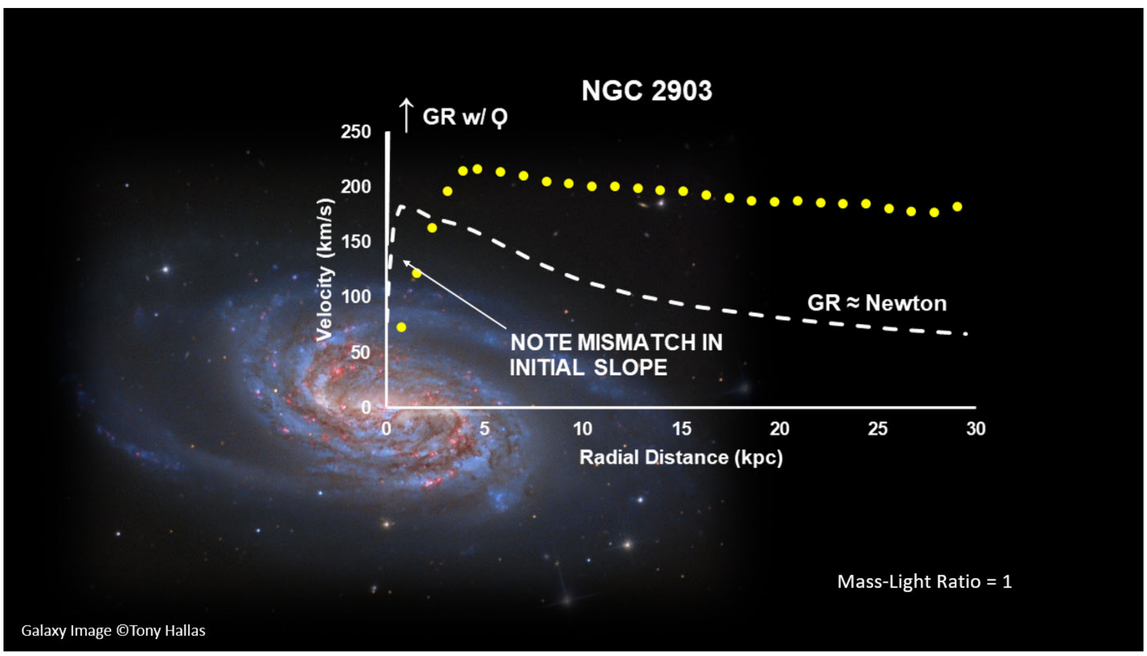

Figure 10. Rotation Curves for NGC 2903 with Mass-to-Light Ratio of 1.0

Surface brightness measurements vary in literature. For example, [25] provides much different brightness values as compared with the referenced work [22]. More work is needed to fetter through the vast amount of literature on surface brightness and velocity rotation curves to verify the surface tension model.

10. Conclusions

The model of spacetime with surface tension acting in the place of "dark matter" correlates well with the shape of measured rotational velocity curves for the three galaxies in this investigation. The model also correlates well in magnitude to measured rotational velocity if a systematic correction is made to the data so that the overall mass-to-light ratio is 1%. The systematic nature of this correction gives merit to the model, but suggests either the current understanding of galaxy formation (bulge stars 100 times brighter than the Sun) or a consistent misinterpretation of the data (correction for absolute versus apparent magnitude).

The apparent gravitation induced by surface tension is insignificant at solar system scales, because it varies with the speed of light squared. However, at galactic scales, surface tension would govern the motion of stars. The contribution of Newton's gravity is minimal for luminous matter within and around galaxies in comparison with surface tension. If this simple theory is correct, it would drastically change the current understanding of galaxy mass, density, evolution, and mechanisms of formation.

X. References

[1] Goenner, H. F. M. (2004) "On the History of Unified Field Theories", *Living Reviews in Relativity*, Volume 7, Issue 2, Max Plank Society, Germany

[2] Zwiebach, B (2009) A First Course in String Theory, 2nd Edition (Cambridge: Cambridge University Press)

[3] Mikhaylov, V. and Witten, E. (2015) "Branes and Supergroups", *Communications in Mathematical Physics*, No. 340, Springer, pp. 699-832

[4] Stueckelberg, E.C.G. (1941) *Helvetica Physica Acta*, Vol. 14, pp. 51-80

[5] Horwitz, L.P. and Oron, O. (2004) "Classical Gravity as an Eikonal Approximation to a Manifestly Lorentz Covariant Quantum Theory with Brownian Interpretation", Relativity, Gravitation, Cosmology, V.V. Dvoeglazov and A.A. Espinoza Garrido, Eds., Nova Science

[6] Land, M.C., Shnerb, N., and Horwitz, L.P. (1995) "On Feynman's Approach to the Foundations of Gauge Theory", *Journal of Mathematical Physics*, Vol. 36, No. 7, pp. 3263-3288

[7] Nelson, E. (2012) "Review of Stochastic Mechanics", Emergent Quantum Mechanics 2011, *Journal of Physics: Conference Series*, 361, 012011, IOP Publishing

[8] Perko, H.A. (2017) "Introducing Surface Tension to Spacetime", IARD2016, *Journal of Physics: Conference Series*, Series 845, IOP Publishing, Ltd.

[9] Perko, H.A. (2017) "Surface Tension of Spacetime", Session H3: New Directions in Gravity, Vol. 62, No. 1, APS April Meeting, Washington, DC, American Physical Society

[10] Perko, H.A. (2019) "Gravitation in the Surface Tension Model of Spacetime", IARD2018, *Journal of Physics: Conference Series*, Series 1239, IOP Publishing, Ltd.

[11] Perko, H.A. (2019) "Hypersurface Tension: A Mechanical Model of Spacetime with Gravitation and Quantum Geometry", Session Z13: General Physics, Vol. 64, No. 3, APS April Meeting, Denver, CO, American Physical Society

[12] Perko, H.A. (2019) "Geometry of Surface Tension", 22nd Eastern Gravity Meeting, DGRAV, APS Division of Gravitational Physics, UMass Dartmouth

[13] O'Brien, J.G. et al. (2017) "Recent Advancements in Conformal Gravity", IARD2016, *Journal of Physics: Conference Series*, Series 845, IOP Publishing, Ltd.

[14] Böhmer, C.G. and Tamanini, N. (2013) "A New Approach to Modifying Theories of Gravity", *Foundations of Physics*, 43, pp. 1478-1488

[15] Battye, R. and Moss, A. (2009) "Anisotropic Dark Energy and CMB Anomalies", *Physics Review D*, 80:023531

[16] Yahalom, A. (2019) "The Effect of Retardation on Galactic Rotation Curves", IARD2018, *Journal of Physics: Conference Series*, Series 1239, IOP Publishing, Ltd.

[17] Milgrom, M. (1983) "A Modification of the Newtonian Dynamics as a Possible Alternative to the Hidden Mass Hypothesis", *Astrophysical Journal*, 270, pp. 365-370

[18] Adamson, A.W. (1990) Physical Chemistry of Surfaces, 5th Edition, Wiley Interscience, New York

[19] Mannheim, P.D. (2005) "Alternatives to Dark Matter and Dark Energy", *The Astrophysical Journal*, 0505266v2

[20] Einstein, A. (1916) "The Foundation of the General Theory of Relativity", *The Collected Papers of Albert Einstein*, Volume 6, A.J. Kox, M.J. Klein, and R. Schulmann Eds., Princeton University Press, New Jersey, 1997

[21] O'Brien, J.G. (2020) Personal Communication

[22] Corbelli, E., et al. (2018) "A Wide-Field H1 Mosaic of Messier 31, The Disk Warp, Rotation, and the Dark Matter Halo", *Astronomy & Astrophysics*, No. ec.m31

[23] de Blok, W.J.G., et al. (2008) "High-Resolution Rotation Curves and Galaxy Mass Models from THINGS", *The Astrophysical Journal*, Vol. 136, No. 6, IOP Publishing, pp. 2648-2719

[24] Courteau, S., et al. (2011) "The Luminosity Profile and Structural Parameters of the Andromeda Galaxy", *The Astrophysical Journal*, 739:20

[25] Willmer, C. N. A. (2018) "The Absolute Magnitude of the Sun in Several Filters", *The Astrophysical Journal Supplement Series*, 23:47, The American Astronomical Society